Cell-Surface Labeling and Internalization by a Fluorescent Inhibitor of Prostate-Specific Membrane Antigen

Tiancheng Liu, Lisa Y. Wu, Marat Kazak, and Clifford E. Berkman*

Department of Chemistry, Washington State University, Pullman, Washington

BACKROUND . Prostate-specific membrane antigen (PSMA) remains an attractive target for imaging and therapeutic applications for prostate cancer. Recent efforts have been made to conjugate inhibitors of PSMA with imaging agents. Compared to antibodies, small-molecule inhibitors of PSMA possess apparent advantages for in vivo applications. To date, there are no reports on the cellular fate of such constructs once bound the extracellular domain of PSMA. The present study was focused on precisely defining the binding specificity, time-dependent internalization, cellular localization, and retention of inhibitor conjugates targeted to PSMA on LNCaP cells. A novel fluorescent inhibitor was prepared as a model to examine these processes.
METHODS. Fluorescence microscopy of LNCaP and PC-3 cell lines was used to monitor the specificity, time-dependent internalization, cellular localization, and retention of a fluorescent PSMA inhibitor.
RESULTS. Fluorescent inhibitor **2** was found to be a potent inhibitor ($IC_{50} = 0.35$ nM) of purified PSMA. Its high affinity for PSMA on living cells was confirmed by antibody blocking and competitive binding experiments. Specificity for LNCaP cells was demonstrated as no labeling by **2** was observed for negative control PC-3 cells. Internalization of **2** by viable LNCaP cells was detected after 30 min incubation at 37°C, followed by accumulation in the perinuclear endosomes. It was noted that internalized fluorescent inhibitor can be retained within endosomes for up to 150 min without loss of signal.
CONCLUSIONS. Our results suggest that potent, small-molecule inhibitors of PSMA can be utilized as carriers for targeted delivery for prostate cancer for future imaging and therapeutic applications. *Prostate 68: 955–964, 2008.* © 2008 Wiley-Liss, Inc.

KEY WORDS: **PSMA; phosphoramidate; fluorescence microscopy; LNCaP; prostate cancer**

INTRODUCTION

The cell-surface enzyme prostate-specific membrane antigen (PSMA) is an important biomarker and target in prostate cancer research. PSMA is up-regulated and strongly expressed on prostate cancer cells, including those that are metastatic [1]. Endothelial- expression of PSMA in the neovasculature of a variety of non-prostatic solid malignancies has also been detected [2,3]. As a consequence, PSMA has attracted significant attention as a target for the delivery of imaging [4–16] and therapeutic agents [17–20]. Unique enzymatic activities have been identified for PSMA and various chemical scaffolds have been developed as inhibitors of this enzyme [21–33].

The employment of PSMA inhibitors as delivery vehicles for imaging agents can serve as an alternative to the more conventional biomarker-targeting approach using antibodies. Indeed, some notable progress

Grant sponsor: National Institutes of Health; Grant number: S06-GM052588; Grant sponsor: National Cancer Institute; Grant number: 1R21CA122126-01; Grant sponsor: Department of Defense; Grant number: W81XWH-06-1-0039.

*Correspondence to: Clifford E. Berkman, Department of Chemistry, Washington State University, Pullman, WA 99164-4630.
E-mail: cberkman@wsu.edu

Received 14 November 2007; Accepted 25 January 2008
DOI 10.1002/pros.20753
Published online 24 March 2008 in Wiley InterScience (www.interscience.wiley.com).

has been made in this area. Tenniswood's group has demonstrated that their phosphinate-based GCP II inhibitors containing a fluorescent group could bind to the membrane of viable LNCaP cells as monitored by fluorescent microscopy [34]. Pomper's group has used urea-based GCP II inhibitors labeled with ^{11}C and ^{125}I to image PSMA-positive lesions in xenograft models of prostate cancer using positron emission tomography (PET) and single photon emission computed tomography (SPECT), respectively [8,13]. Slusher and coworkers developed a near-infrared (NIR) fluorescent dye-inhibitor conjugate for in vitro imaging of endogenous and ectopically expressed PSMA in human cells as well as in vivo imaging of xenogrft tumors [11]. These studies not only confirm that GCP II inhibitor conjugates can be effectively applied for prostate cancer imaging, but also support the concept that GCP II inhibitors may serve as carriers for chemotherapeutic agents targeted to PSMA-expressing tumors. In fact, Kozikowski's group prepared a urea-based GCP II inhibitor-doxorubicin conjugate for targeting the prostate cancer cells [35]. Although the conjugate still retained potent GCP II inhibitor activity, it exhibited poor anti-tumor activity in PSMA-positive C4–2 cells. It was speculated that the conjugate is not undergoing the appropriate enzymatic processing required to release doxorubicin intracellularly.

Although there has been progress in imaging and therapeutic applications with GCP II inhibitor conjugates, the mechanisms of cellular uptake, internalization, and retention of such constructs by prostate cancer cells have yet to be determined. In our present study, we fluorescently labeled a phosphoramidate peptidomimetic inhibitor **1** (Fig. 1) of PSMA with an amine-reactive fluorescein reagent and examined the cellular specificity as well as internalization of this dye-inhibitor conjugate **2**.

MATERIALS AND METHODS

Cell Lines, Reagents, and General Procedures

LNCaP and PC3 cells were obtained from the American Type Culture Collection (Manassas, VA). The monoclonal antibody 3C6 was obtained from Northwest Biotherapeutics (Seattle, WA). Tetramethylrhodamine-6-isothiocyanate (6-TRITC; R isomer) and transferrin-Texas Red were obtained from Invitrogen–Molecular Probes. All other chemicals and cell-culture reagents were purchased from Fisher Scientific (Sommerville, NJ), Pierce (Rockford, IL), or Sigma–Aldrich (St. Louis, MO). All solvents used in chemical reactions and triethylamine (TEA) were anhydrous and obtained as such from commercial sources. Aqueous solutions were prepared with deionized distilled water (Milli-Q water system, Millipore, Bedford, MA). All other reagents were used as supplied unless otherwise stated. Liquid flash chromatography (silica or C18) was carried out using a Biotage 12i/40i system. ^{1}H, ^{13}C, and ^{31}P NMR spectra were recorded on a Bruker DRX 300 MHz and 500 MHz NMR Spectrometer. ^{1}H NMR chemical shifts are relative to TMS ($\delta = 0.00$ ppm), $CDCl_3$ ($\delta = 7.26$ ppm), or D_2O ($\delta = 4.87$). ^{13}C NMR chemical shifts are relative to $CDCl_3$ ($\delta = 77.23$ ppm). ^{31}P NMR chemical shifts in $CDCl_3$, or D_2O were externally referenced to 85% H_3PO_4 ($\delta = 0.00$ ppm) in $CDCl_3$, and D_2O, respectively.

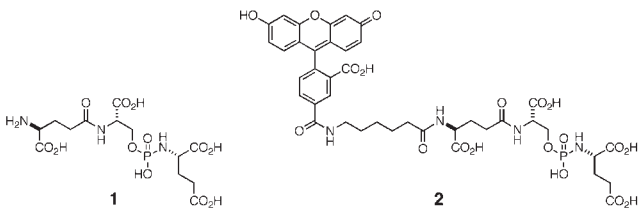

Fig. 1. Structures of peptidomimetic inhibitor **1** and its fluorescent conjugate **2**.

Preparation of Phosphoramidate Peptidomimetic Inhibitor

2-Benzyloxycarbonylamino-4-(1-benzyloxycarbonyl-2-hydroxy-ethylcarbamoyl)-butyric acid benzyl ester (3). TEA (765 μl, 2.04 equiv) was added via syringe to a stirred solution of Z-Glu-OBn (1 g, 2.7 mmol), L-serine benzyl ester (655 mg. 1.05 equiv) and HBTU (1.12 g, 1.1 equiv) in anhydrous DMF (35 ml). The reaction mixture was stirred for 1.5 hr at room temperature. The reaction mixture was washed with 10% HCl (50 ml) and the crude mixture was extracted with EtOAc (50 ml). The organic layer was sequentially washed with 10% $NaHCO_3$ (50 ml) and brine (50 ml). After drying the organic layer with $MgSO_4$, the solvent was removed in vacuo to yield the white solid. Yield 96.3% M.P (104–106°C). ^{1}H NMR (500 MHz, $CDCl_3$): δ 1.73–1.78 (m, 1H), 2.19–2.25 (m, 1H), 2.35–2.44 (m, 2H), 3.45–3.48 (t, 1H, J = 7 Hz), 3.94–3.98 (m, 1H), 4.05–4.09 (m, 1H), 4.44–4.47 (m, 1H), 4.70–4.71 (m, 1H), 5.09–5.25 (m, 6H), 5.59–5.61 (d, 1H, J = 9Hz), 6.44–6.45 (d, 1H, J = 7 Hz), 7.28–7.41 (m, 15H). ^{13}C NMR (75 MHz, $CDCl_3$): δ 29.1, 32.3, 53.6, 55.7, 63.4, 68.1, 128.7, 128.9, 135.7, 135.8, 136.5, 157.1, 171.1, 172.2, 172.6.

2-{Benzyloxy-[2-benzyloxycarbonyl-2-(4-benzyloxycarbonyl-4-benzyloxycarbonylamino-butyrylamino)-ethoxy]-phosphorylamino}-pentanedioic acid dibenzyl ester (6). TEA (418 μl, 3 equiv) and benzyl alcohol (310 μl, 3 equiv) were sequentially added dropwise to a stirred solution of bis(diisopropylamino) chlorophosphine (797 mg, 3 equiv) in anhydrous CH_2Cl_2 (5 ml). The

reaction mixture was stirred for 10 min at 0°C and 1 hr at room temperature. The residue was transferred via syringe to a stirred solution of alcohol **3** (548 mg, 1 equiv) and *N,N*-diisopropylammonium tetrazolide (179 mg, 1.05 equiv) in CH_2Cl_2 (20 ml) at 0°C under $argon_{(g)}$. The reaction mixture was stirred for 3 hr at room temperature, after which the solvent was removed in vacuo. The crude reaction mixture was dissolved in CH_3CN (30 ml) and cooled to 0°C. A solution of 5-ethylthio-1*H*-tetrazole (143 mg, 1.1 equiv) in a mixture of distilled H_2O (1 ml) and CH_3CN (1 ml) was then added and the reaction mixture stirred for 10 min at 0°C and then 1 hr at room temperature. The solvent was removed in vacuo, the residue was washed with 10% HCl (50 ml), and the crude mixture was extracted with EtOAc (50 ml). The organic layer was sequentially washed with 10% $NaHCO_3$ (50 ml), distilled H_2O (50 ml), and brine (50 ml). After drying the organic layer with $MgSO_4$, the solvent was removed in vacuo to yield the phosphite **5** as an oil, which was used immediately in the next step without characterization or purification. A solution of glutamic acid dibenzyl ester (0.649 g, 1.3 mmol) in CH_3CN (6 ml) and TEA (362 μl, 2.6 equiv) was added dropwise to a stirred solution of crude phosphite **5** (1 equiv) in CH_3CN (3 ml) and CCl_4 (6 ml) at 0°C under argon. The reaction mixture was stirred 2 hr and solvent was reduced to half its volume in vacuo. The residue was dissolved in CH_2Cl_2 (40 ml) and sequentially washed with 10% HCl (2 × 40 ml), 10% $NaHCO_3$ (40 ml), and brine (40 ml). The organic layer was dried over $MgSO_4$ and concentrated in vacuo to give a yellow oil. The product was isolated by flash chromatography C18 (3:7 water:acetonitrile). Rf = 0.17, Yield (17.0%). ^{1}H NMR (300 MHz, $CDCl_3$): δ 1.82–1.88 (m, 1H), 1.98–2.09 (m, 2H), 2.19–2.32 (m, 5H), 3.57–3.71 (m, 1H), 3.81–3.90 (m, 1H), 4.16–4.19 (m, 1H), 4.28–4.29 (m, 1H), 4.32–4.37 (m, 1H), 4.74–4.84 (m, 1H), 4.86–4.87 (m, 2H), 4.95–5.13(m, 10H), 5.92–5.94 (d, 1/2H, J = 4 Hz), 6.18–6.19 (d, 1/2H, J = 4 Hz), 7.09–7.10 (d, 1/2H, J = 4 Hz), 7.14–7.45 (m, 31.5 H). ^{13}C NMR (75 MHz, $CDCl_3$): δ 27.9, 29.5, 29.7, 30.2, 30.3, 32.3, 53.3, 53.5, 54.2, 66.9, 67.1, 67.2, 67.4, 67.5, 67.7, 68.0, 68.1, 69.0, 128.3, 128.4, 128.5, 128.6, 128.7, 128.8, 128.9, 129.0, 129.1, 129.2, 135.6, 135.7, 135.8, 135.9, 136.0, 136.2, 136.3, 136.4, 136.5, 136.9, 137.0, 156.8, 169.5, 169.6, 172.5, 172.6, 172.7, 172.9, 173.0, 173.1, 173.3. ^{31}P NMR (300 MHz, $CDCl_3$): δ 8.55 and 8.96.

2-{[2-(4-Amino-4-carboxy-butyrylamino)-2-carboxy-ethoxy]-hydroxy-phosphorylamino}-pentanedioic acid pentapotassium salt (1). To a solution of a benzyl ester protected phosphoramidate **6** (71 mg, 0.069 mmol) in THF (1.5 ml), was added 10% Pd/C (12 mg), K_2CO_3 (23 mg, 2 equiv) and distilled H_2O (1 ml). The mixture was stirred vigorously, purged with $argon_{(g)}$ and then charged with $H_{2(g)}$ under balloon pressure for 7 hr at room temperature. The solvent was removed in vacuo and the residue was dissolved in 1:1 methanol:water, and filtered through a 0.2 μm PTFE micropore filtration disk (Whatman). The solvent was removed in vacuo to yield solid (**1**). Yield (89.9%). ^{1}H NMR (300 MHz, D_2O): δ 1.75–1.94 (m, 2H), 1.98–2.10 (m, 2H), 2.12–2.20 (m, 2H), 2.43–2.51 (m, 2H), 3.47–3.54 (q, 1H, J = 6 Hz, 15 Hz), 3.63–3.67 (q, 1H, J = 5 Hz, 8 Hz), 3.98–4.10 (m, 2H), 4.32–4.35 (t, 1H, J = 4 Hz). ^{13}C NMR (75 MHz, D_2O): δ 26.8, 31.4, 31.7, 31.8, 33.7, 48.7, 54.2, 55.6, 55.8, 56.6, 64.6, 64.7, 174.3, 175.21, 176.0, 181.5, 181.6, 182.9. ^{31}P NMR (300 MHz, D_2O): δ 7.63.

Preparation of Fluorescent Inhibitor Conjugate

A solution of 5-FAM-X, SE (4 μmol) in 100 μl DMSO was added to a stirred solution of the inhibitor core (2 μmol, 100 μl of 20 mM in H_2O), 160 μl H_2O, 40 μl of 1 M $NaHCO_3$, which were stirred for 6 hr. The pH of the solution was then adjusted to 9.3 by an addition of 8 μl of 1 M Na_2CO_3. 25 mg of Si-Isocyanate resin (SiliCycle, Inc., Quebec, Canada) was added to the solution to scavenge the unreacted inhibitor core **1** by stirring overnight at room temperature. The solution was subsequently centrifuged (9,000 rpm, 10 min) and the supernatant was lyophilized in a 2 ml microcentrifuge tube. Unreacted or hydrolyzed 5-FAM-X, SE was removed by successively triturating the lyophilized solid 10 times with 1 ml portions of DMSO and centrifuging the mixture (1 min at 13,000 rpm) after each wash. The fluorescein-conjugated inhibitor was resuspended in 50 mM Tris buffer (pH 7.5) to give a final concentration of 2 mM (approximately 800 μl).

IC50 Determination for Inhibitor Core and Fluorescent Conjugate

Inhibition studies were performed as described previously with only minor modifications [21,36]. Working solutions of the substrate (*N*-[4-(phenylazo)-benzoyl]-glutamyl-*g*-glutamic acid, PABGgG) and inhibitors were made in TRIS buffer (50 mM, pH 7.4 containing 1% Triton X-100). Working solutions of purified PSMA were diluted in TRIS buffer (50 mM, pH 7.4 containing 1% Triton X-100) to provide from 15% to 20% conversion of substrate to product in the absence of inhibitor. A typical incubation mixture (final volume 250 μl) was prepared by the addition of either 25 μl of an inhibitor solution or 25 μl TRIS buffer (50 mM, pH 7.4 containing 1% Triton X-100) to 175 μl TRIS buffer (50 mM, pH 7.4 containing 1% Triton X-100) in a test tube. PABGγG (25 μl, 100 μM) was added to the above solution. The enzymatic reaction was initiated by the addition of 25 μl of the PSMA working solution. In all

cases, the final concentration of PABGγG was 10 μM while the enzyme was incubated with five serially diluted inhibitor concentrations providing a range of inhibition from 10% to 90%. The reaction was allowed to proceed for 15 min with constant shaking at 37°C and was terminated by the addition of 25 μl methanolic TFA (2% trifluoroacetic acid by volume in methanol) followed by vortexing. The quenched incubation mixture was quickly buffered by the addition of 25 μl K_2HPO_4 (0.1 M), vortexed, and centrifuged (10 min at 7,000*g*). An 85 μl aliquot of the resulting supernatant was subsequently quantified by HPLC as previously described [26,37]. IC_{50} values were calculated using KaleidaGraph 3.6 (Synergy Software).

Conjugation of Fluorescent Dyes to Monoclonal Antibody

The monoclonal antibody 3C6 (1 mg/ml, in PBS with 0.02% NaN_3) was first dialyzed against PBS at 4°C overnight to removal NaN_3, and then concentrated up to 5 mg/ml. To a 50 ml round bottom flask was sequentially added 200 μl of 3C6 (5 mg/ml), 110 μl of H_2O, and 40 μl of a freshly prepared mixture of 1 M $NaHCO_3$:1 M Na_2CO_3 (5:1 v:v ratio, pH 9.3). Tetramethylrhodamine-6-isothiocyanate (1 mg) was dissolved in 50 μl of DMSO and added dropwise to the reaction mixture with constant stirring. The reaction mixture was stirred for 1 hr in the dark at room temperature. The labeled antibody was then washed in 2 ml of PBS six times and after each wash, the free dyes were removed by centrifugal filtration (Centricon YM-30; Millipore). The final solution of fluorescently labeled 3C6 (1 mg/ml) was stored in PBS containing 0.02% NaN_3, at 4°C, and protected from light.

Cell Surface Labeling and Internalization Studies

PSMA-positive cells (LNCaP) and PSMA-negative cells (PC-3) were grown in T-75 flasks with complete growth medium [RPMI 1640 containing 10% heat-inactivated fetal calf serum (FBS), 100 units of penicillin and 100 μg/ml streptomycin] in a humidified incubator at 37°C and 5% CO_2. Confluent cells were detached with 0.25% trypsin-0.53 mM EDTA solution, harvested, and plated in 2-well slide chambers at a density of 4×10^4 cells/well. Cells were grown for 3–4 days before conducting the following experiments.

Cell-labeling with fluorescent inhibitor 2 and competitive binding experiments. Cells grown on the slides were first washed twice with warm medium A (phosphate-free RPMI 1640 containing 1% FBS, 0.1% NaN_3), then incubated with 1 ml of fluorescent inhibitor (4 μM) in warm medium A for 30 min at room temperature. In competitive binding experiments, cells were pre-incubated for 30 min with 1 ml of inhibitor core **1** (80 μM).

Inhibitor-antibody blocking experiments. Cells were pre-incubated with either 1 ml of fluorescent inhibitor **2** (4 μM) or 1 ml of TRITC-conjugated antibody 3C6 (500-fold dilution) for 30 min at room temperature. Cells pre-treated with fluorescent inhibitor **2** were then treated with TRITC-conjugated antibody 3C6 (500-fold dilution) for another 30 min at room temperature, correspondingly, those cells that were pre-treated with TRITC-conjugated antibody 3C6 were then treated with fluorescent inhibitor **2** for another 30 min.

Time-dependent internalization of fluorescent inhibitor 2. Cells were first washed twice with cold medium B (phosphate-free RPMI 1640 containing 1% FBS), incubated with 1 ml of fluorescent inhibitor **2** (4 μM) in cold medium B for 1 hr at 4°C, and then washed twice with cold medium B. The medium was then replaced with pre-warmed medium C (phosphate-free RPMI 1640 containing 10% FBS) and cells were incubated for various lengths of times (0, 30, 60, 90, 120, 150 min) in a humidified incubator at 37°C and 5% CO_2.

Localization of internalized fluorescent inhibitor 2. Cells were first washed twice with cold medium B (phosphate-free RPMI 1640 containing 1% FBS), incubated with 1 ml of fluorescent inhibitor **2** (4 μM) in cold medium B for 1 hr at 4°C, and then washed twice with cold medium B. The medium was then replaced with pre-warmed medium C (phosphate-free RPMI 1640 containing 10% FBS) and cells were incubated for 1 hr at 37°C (5% CO_2). The cell medium was replaced with pre-warmed medium C containing tranferrin-Texas Red conjugate (20 μg/ml) and incubated for another 60 min at 37°C (5% CO_2).

All the above treated cells were washed twice with KRB buffer pH 7.4 (mmol/L: NaCl 154.0, KCl 5.0, $CaCl_2$ 2.0, $MgCl_2$ 1.0, HEPES 5.0, D-glucose 5.0), fixed with 4% paraformaldehyde, counterstained with DAPI (according to manufacturer's instructions; Invitrogen), and mounted for microscopy. Cells were visualized using a Nikon E600 Fluorescence Microscope with filters for fluorescein (excitation: 450–490, emission: 510–550BP, exposure time: 800 mS), TRITC (excitation: 530–560, emission: 590–650BP, exposure time: 800 mS), and DAPI (excitation: 330–380, emission: 435LP, exposure time: 20 mS). Images were captured and merged using the ''SPOT advanced'' software 4.6, and edited by National Institutes of Health (NIH) Image J software (http://rsb.info.nih.gov/ij/) and Adobe Photoshop CS2.

RESULTS

Preparation of Fluorescent PSMA Inhibitor 2

Fluorescently labeled PSMA inhibitor **2** was prepared as described in Scheme 1. Starting with bis-(diisopropylamino) chlorophosphine, the precursor to inhibitor core **1** was generated using methodology recently developed in our lab [21]. Hydrogenolysis buffered with potassium bicabonate resulted in the deprotection of the CBZ group and benzyl esters to provide the phosphoramidate inhibitor core **1**. Conjugation of inhibitor core **1** with the *N*-hydroxysuccinimide ester of 5-FAM-X under conditions typical for peptide or protein labeling provided the fluorescent inhibitor conjugate **2**.

Selective Binding to PSMA on Prostate Cancer Cells

We first confirmed that both the inhibitor core **1** and the fluorescent inhibitor conjugate **2** were potent inhibitors of PSMA using an HPLC-based assay previously developed by our group [21,26,37]. The IC_{50} values for inhibitor core **1** and fluorescent inhibitor conjugate **2** against PSMA purified from LNCaP cells [38] were 14 and 0.35 nM, respectively. Dye-conjugation of the inhibitor core resulted in a structure with greater inhibitory potency against PSMA. We have noticed a similar trend with related phosphoramidate inhibitor cores when compared to their *N*-acyl analogs (unpublished data).

To determine that fluorescent inhibitor conjugate **2** retained its high affinity for PSMA on living cells, both PSMA-positive (LNCaP) and PSMA-negative (PC-3) cells were treated with fluorescent inhibitor conjugate **2**. Fluorescence microscopy revealed that the surface of LNCaP cells was fluorescently labeled with **2** while no labeling was observed on the surface of PC-3 cells (Fig. 2A,C). The intensity of the fluorescence signal due to cell labeling with **2** was decreased significantly when LNCaP cells were pre-treated with inhibitor core **1** (Fig. 2A,B), thus supporting the conclusion that cell labeling by **2** was due to binding to PSMA.

To further confirm that fluorescent inhibitor conjugate **2** was in fact targeting PSMA on the surface of LNCaP cells, co-localization experiments were conducted using the monoclonal antibody 3C6 conjugated to TRITC (3C6-TRITC). The mAb 3C6 recognizes a conformational epitope on the extracellular domain of PSMA [39]. LNCaP cells were first treated with 3C6-TRITC and then fluorescent inhibitor conjugate **2**. Likewise, LNCaP cells were first treated with conjugate **2** and then 3C6-TRITC. Surprisingly, both the 3C6-TRITC and fluorescent inhibitor conjugate **2** dramatically reduced the binding of the other (Fig. 3). Pre-incubation with 3C6-TRITC essentially precluded fluorescent inhibitor conjugate **2** from binding to LNCaP cells (Fig. 3C,G). In a contrast, fluorescent inhibitor conjugate **2** only partially blocked 3C6-TRITC from binding to LNCaP cells (Fig. 3F,B) and as the merged picture (Fig. 3H) suggests, fluorescent inhibitor conjugate **2** and 3C6-TRITC co-localize on cellular membranes of LNCaP cells.

Internalization of Fluorescent Inhibitor Conjugate 2

Incubation of LNCaP cells with **2** alone at 4°C resulted in distinct cell membrane labeling (Fig. 4A). Upon warming these cells to 37°C, internalization of **2** was observed to be time dependent (Fig. 4). By 60 min, sparse labeling extended throughout the cytoplasm (Fig. 4C) and by 120 min, intense labeling was focused on the peri-nuclear region (Fig. 4E,F).

To better understand the intracellular fate of **2** once internalized in LNCaP cells, co-localization studies

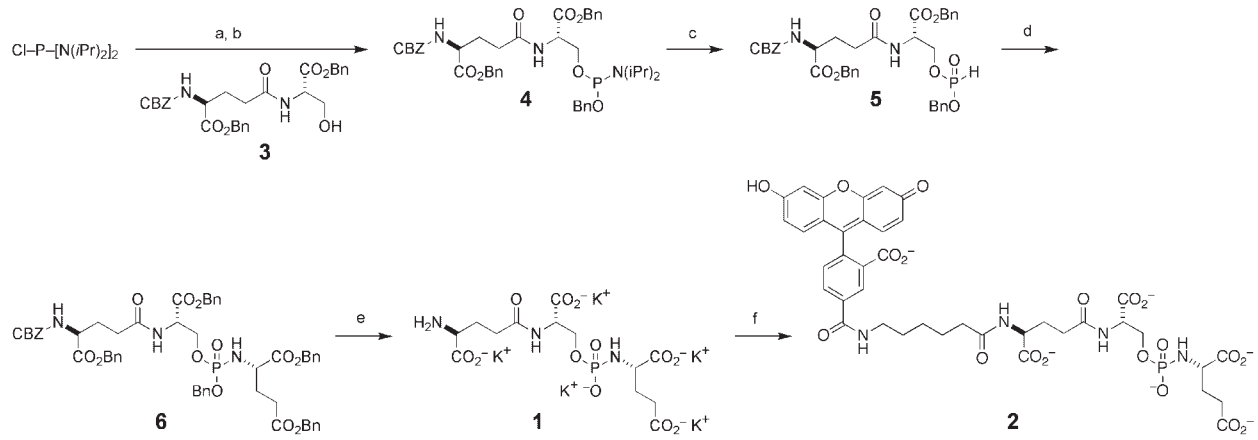

Scheme. 1. Synthesis of fluorescent inhibitor 2. Reagents and conditions: (a) benzyl alcohol (3.0 equiv), TEA (3.0 equiv); CH_2Cl_2, 0°C, 1 hr (b) CBZ-Glu(Ser-OBn)-OBn (1.0 equiv), diisopropylammonium tetrazolide (1.05 equiv), 3 hr, CH_2Cl_2; (c) 5-ethylthio-1*H*-tetrazole (1.0 equiv), CH_3CN, H_2O; (d) CH_3CN, TEA (2.6 equiv), *p*-ToSH H-Glu(OBn)-OBn (1.3 equiv) then CCl_4 (6 ml); (e) H_2, cat. Pd (10% on C), K_2CO_3 (2.0 equiv), THF- H_2O, 7 hr, room temp.; (f) 5-FAM-X SE, DMSO, $NaHCO_3$.

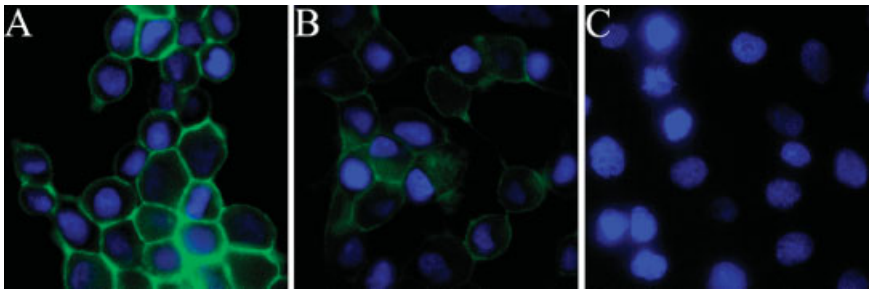

Fig. 2. Selective and competitive binding of **2** to PSMA-positive cells. **A**: Live LNCaP cells labeled with 2 for 30 min at room temperature. **B**: LNCaP cells pretreated with inhibitor core **I** for 30 min at room temperature and then treated with 2 for 30 min at room temperature. **C**: PC-3 cells treated with 2 for 30 min at room temperature as a negative control. All cells were fixed and nuclei stained with DAPI.

were conducted with the subcellular marker, transferrin-Texas Red (endosomal marker). LNCaP cells were pre-incubated with **2** and subsequently incubated with transferrin-Texas Red. Co-localization of internalized **2** with transferrin-Texas Red was visualized as a yellow signal in merged images, and appeared strongly in perinuclear region (Fig. 5A–D).

DISCUSSION

Both **2** and its parent inhibitor core **1** were potent inhibitors of PSMA. Once the inhibitor core **1** was conjugated with 5-FAM-X SE, the fluorescent inhibitor conjugate **2** exhibited enhanced potency against PSMA. These results are not inconsistent with our previously unreported findings in which similar non-acylated peptidomimetic phosphoramidates exhibited over 10-fold weaker inhibitory potency against PSMA compared to intact *N*-benzoyl derivatives. This is not inconsistent with our previous findings in which we confirmed that hydrophobic motifs remote from a zinc-binding group on PSMA inhibitors enhanced inhibitory potency [26].

Cell-labeling experiments demonstrated that fluorescent inhibitor conjugate **2** successfully targeted PSMA-expressing cells and were effective in labeling cell membranes of LNCaP cells. With PC-3 cells, which do not express PSMA no cell-labeling was observed. To confirm that binding of **2** to the surface LNCaP cells was due to interactions with PSMA, competitive binding experiments were conducted in the presence of the inhibitor core **1**. When LNCaP cells were pre-treated with **1**, fluorescence labeling by **2** was decreased significantly as shown in Figure 2B. The binding of fluorescent inhibitor conjugate **2** was also challenged with the fluorescently labeled monoclonal antibody

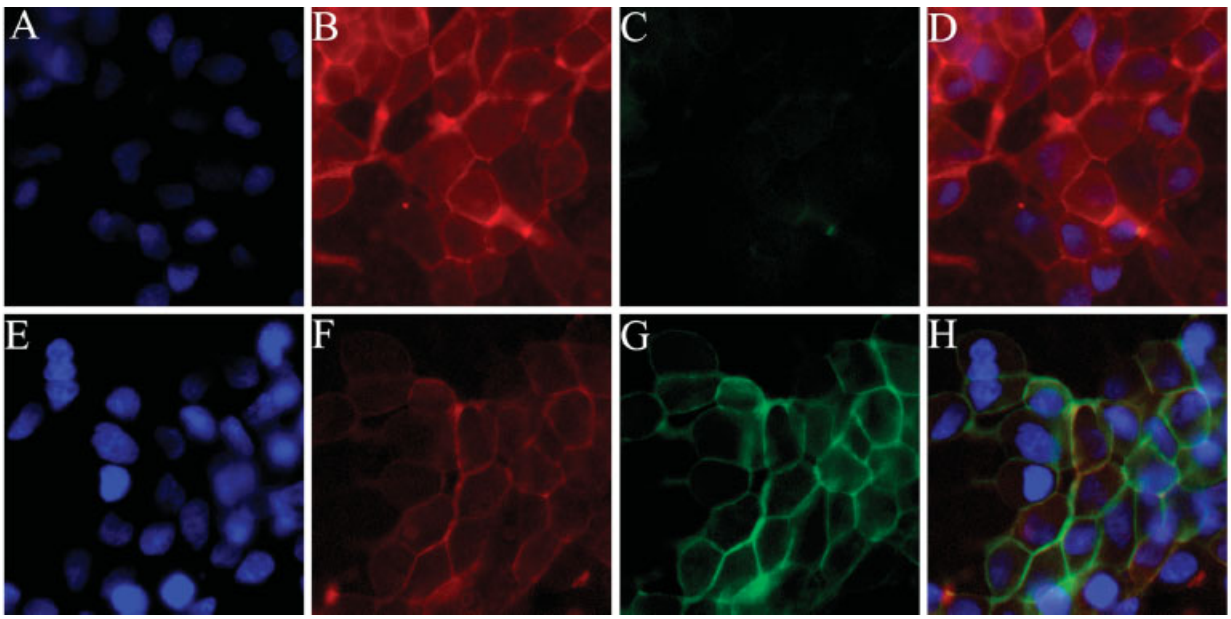

Fig. 3. Co-localization of **2** with mAb 3C6 on the LNCaP cell surfaces. **Top panel**: LNCaP cells were pre-incubated with 3C6 -TRITC, and then incubated with **2** (**A**–**D**). Image D is the result of merging images A–C. **Bottom panel**: LNCaP cells were pre-incubated with **2**, and then incubated with 3C6 -TRITC (**E**–**H**). Image H is the result of merging images in E–G. All cellular nuclei were stained by DAPI.

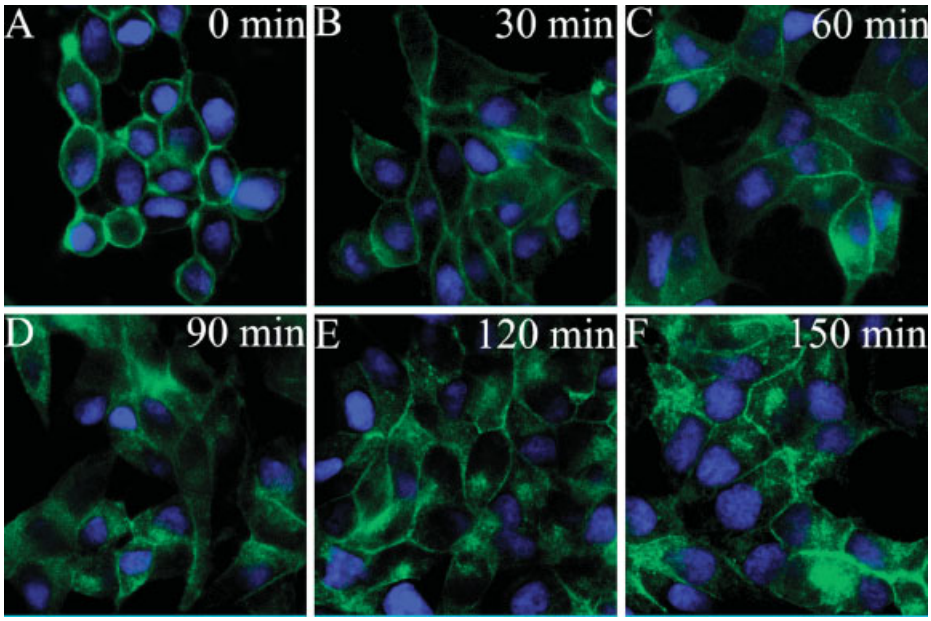

Fig. 4. Time-dependent internalization of 2 in LNCaP cells. Live LNCaP cells labeled with **2** were incubated for 0 (**A**), 30 (**B**), 60 (**C**), 90 (**D**), 120 (**E**), and 150 (**F**) min at 37°C. Cells were then fixed and nuclei stained with DAPI.

3C6-TRITC. When LNCaP cells were first treated with 3C6-TRITC, it essentially precluded the fluorescent inhibitor conjugate **2** from binding to LNCaP cells (Fig. 3C,G). Based on these results we have hypothesized that binding of 3C6 to PSMA either blocks access to the active site directly or causes a global conformation change resulting in an indirect occlusion of the active site. Pre-treatment with **2** only partially reduced 3C6-TRITC binding to LNCaP cells (Fig. 3F,B). In the latter case, merged images of bound 3C6-TRITC and **2** (Fig. 3H) suggest that both cell-labeling agents co-localize on cellular membranes of LNCaP cells. These results demonstrate that fluorescent inhibitor conjugate **2** is a specific labeling agent for PSMA-expressing cells.

After labeling PSMA on LNCaP cell membranes with **2**, internalization of this fluorescent inhibitor conjugate was observed and to be time dependent (Fig. 4). By 60 min, sparse labeling extended throughout the cytoplasm (Fig. 4C) and by 120 min, intense labeling was focused on the peri-nuclear region (Fig. 4E,F). To further identify the intracellular fate of **2** once internalized in LNCaP cells, co-localization studies were conducted with the transferrin-Texas Red as an endosomal marker. Co-localization of internalized **2** with transferrin-Texas Red was detected and appeared greatest in the perinuclear region (Fig. 5A–D). These internalization results are not inconsistent with those previously reported for antibody-bound PSMA [39–41]. It has been recognized that internalization of PSMA occurs through a clathrin-dependent endocytic-mechanism and is constitutive or can be rapidly induced by antibody binding [42]. These previous studies confirmed that internalized PSMA is localized to the

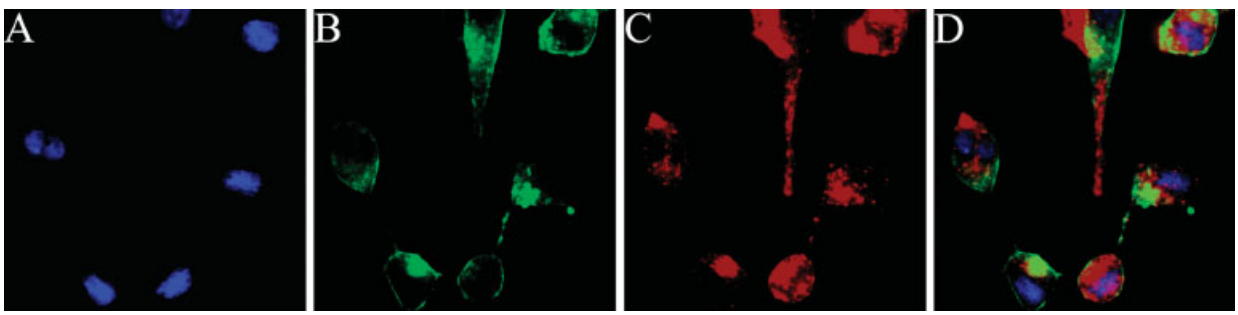

Fig. 5. Co-localizion studies of internalized 2 with transferrin-Texas Red. LNCaP cells were pre-incubated with 2, and then incubated with transferrin-Texas Red (**A**–**D**). Representative images A (DAPI, blue), B (**2**, green), and C (transferrin-Texas Red, red) were merged to obtain image D. Regions of colocalizion of transferrin-Texas Red and **2** appear yellow in merged image D.

recycling endosomal compartment (REC) as proved by its co-localization with internalized transferrin [39–41]. Our data demonstrates that the cellular uptake of fluorescent inhibitor conjugate **2** occurs through the internalization of the inhibitor-PSMA complex, which is retained in endosomes and finally accumulates in perinuclear region.

In general, internalization of the receptor-ligand complex via clathrin-coated pits usually results in an accumulation in endosomes where acidic conditions promotes complex dissociation. The dissociated molecules are either recycled back to the cell surface or targeted to lysosomes for further degradation [43]. For example, this characterizes the fate of transferrin-transferrin receptor (TfR) complex [44–50]. Although PSMA shares a high degree of structural homology with TfR1 [51,52] and their internalization occurs through the same endosomal-pathway, there are significant differences in internalization and recycling rates. Transferrin-TfR 1 complex exhibits rapid internalization, dissociation, and recycling to cell surfaces [49,50]. In contrast, we have found that internalization of **2** bound to PSMA occurs more slowly but is retained longer within cells.

Considering that the enzymatic activity of PSMA is maintained at a wide pH range (5–8) [53–55] and that internalized PSMA must proceed first through early endosomes (~pH 6.0) and then RECs (pH value: 6–7.0) before returning to cellular plasma membrane [56–58], we surmise that under such weakly acidic condition, the PSMA-**2** inhibitor complex is stable and can be retained within endosomes for hours. A previous report estimated that 60% of the cell surface PSMA was constitutively internalized and retained in cells for over 6 hr [42]. Therefore, it is likely that the specificity of **2** for PSMA and its propensity to be internalized can be harnessed to deliver therapeutic agents that do not require dissociation from the enzyme-inhibitor complex to exert their therapeutic effect. In summary, the results described herein confirm that targeted delivery to prostate cancer cells may be achieved by small molecules such as phosphoramidate peptidomimetics and serve as an alternative to antibody-based approaches.

ACKNOWLEDGMENTS

This work was supported in part the National Institutes of Health, MBRS SCORE Program-NIGMS (S06-GM052588), the National Cancer Institute (1R21CA122126-01) and the Department of Defense (W81XWH-06-1-0039). The authors would also like to extend their gratitude to W. Tam and the NMR facility at San Francisco State University and M. Holroyd for editorial assistance.

REFERENCES

1. Bacich DJ, Pinto JT, Tong WP, Heston WD. Cloning, expression, genomic localization, and enzymatic activities of the mouse homolog of prostate-specific membrane antigen/NAALADase/folate hydrolase. Mamm Genome 2001;12(2):117–123.
2. Chang SS, O'Keefe DS, Bacich DJ, Reuter VE, Heston WD, Gaudin PB. Prostate-specific membrane antigen is produced in tumor-associated neovasculature. Clin Cancer Res 1999;5(10): 2674–2681.
3. Chang SS, Reuter VE, Heston WD, Gaudin PB. Department of Urologic Surgery VUMCNTUSA. Comparison of anti-prostate-specific membrane antigen antibodies and other immunomarkers in metastatic prostate carcinoma. Urology 2001;57(6): 1179–1183.
4. Rosenthal SA, Haseman MK, Polascik TJ. Division of Radiation Oncology RAoSMGICUSA. Utility of capromab pendetide (ProstaScint) imaging in the management of prostate cancer. Tech Urol 2001;7(1):27–37.
5. Bander NH, Milowsky MI, Nanus DM, Kostakoglu L, Vallabhajosula S, Goldsmith SJ. Phase I trial of 177lutetium-labeled J591, a monoclonal antibody to prostate-specific membrane antigen, in patients with androgen-independent prostate cancer. J Clin Oncol 2005;23(21):4591–4601.
6. Chu TC, Shieh F, Lavery LA, Levy M, Richards-Kortum R, Korgel BA, Ellington AD. Labeling tumor cells with fluorescent nanocrystal-aptamer bioconjugates. Biosens Bioelectron 2006; 21(10):1859–1866.
7. Farokhzad OC, Khademhosseini A, Jon S, Hermmann A, Cheng J, Chin C, Kiselyuk A, Teply B, Eng G, Langer R. Microfluidic system for studying the interaction of nanoparticles and microparticles with cells. Anal Chem 2005;77(17):5453–5459.
8. Foss CA, Mease RC, Fan H, Wang Y, Ravert HT, Dannals RF, Olszewski RT, Heston WD, Kozikowski AP, Pomper MG. Radiolabeled small-molecule ligands for prostate-specific membrane antigen: In vivo imaging in experimental models of prostate cancer. Clin Cancer Res 2005;11(11):4022–4028.
9. Gao X, Cui Y, Levenson RM, Chung LW, Nie S. In vivo cancer targeting and imaging with semiconductor quantum dots. Nat Biotechnol 2004;22(8):969–976.
10. Guilarte TR, McGlothan JL, Foss CA, Zhou J, Heston WD, Kozikowski AP, Pomper MG. Department of Environmental Health Sciences JHSoPHBMDUSA. Glutamate carboxypeptidase II levels in rodent brain using [125I]DCIT quantitative autoradiography. Neurosci Lett 2005;387(3):141–144.
11. Humblet V, Lapidus R, Williams LR, Tsukamoto T, Rojas C, Majer P, Hin B, Ohnishi S, De Grand AM, Zaheer A, Renze JT, Nakayama A, Slusher BS, Frangioni JV. High-affinity near-infrared fluorescent small-molecule contrast agents for in vivo imaging of prostate-specific membrane antigen. Mol Imaging 2005;4(4):448–462.
12. Milowsky MI, Nanus DM, Kostakoglu L, Sheehan CE, Vallabhajosula S, Goldsmith SJ, Ross JS, Bander NH. Vascular targeted therapy with anti-prostate-specific membrane antigen monoclonal antibody J591 in advanced solid tumors. J Clin Oncol 2007;25(5):540–547.
13. Pomper MG, Musachio JL, Zhang J, Scheffel U, Zhou Y, Hilton J, Maini A, Dannals RF, Wong DF, Kozikowski AP. 11C-MCG: Synthesis, uptake selectivity, and primate PET of a probe for glutamate carboxypeptidase II (NAALADase). Mol Imaging 2002;1(2):96–101.
14. Smith MR, Nelson JB. Future therapies in hormone-refractory prostate cancer. Urology 2005;65(5 Suppl):9–16, discussion 17.

15. Smith-Jones PM, Vallabhajosula S, Navarro V, Bastidas D, Goldsmith SJ, Bander NH. Radiolabeled monoclonal antibodies specific to the extracellular domain of prostate-specific membrane antigen: Preclinical studies in nude mice bearing LNCaP human prostate tumor. J Nucl Med 2003;44(4):610–617.
16. Tsukamoto T, Wozniak KM, Slusher BS. Progress in the discovery and development of glutamate carboxypeptidase II inhibitors. Drug Discov Today 2007;12(17–18):767–776.
17. Tasch J, Gong M, Sadelain M, Heston WD. Department of Urology MHMS-KCCNYNYUSA. A unique folate hydrolase, prostate-specific membrane antigen (PSMA): A target for immunotherapy? Crit Rev Immunol 2001;21(1–3):249–261.
18. Salit RB, Kast WM, Velders MP. Ins and outs of clinical trials with peptide-based vaccines. Front Biosci 2002; 7:e204–213.
19. Lu J, Celis E. Recognition of prostate tumor cells by cytotoxic T lymphocytes specific for prostate-specific membrane antigen. Cancer Res 2002;62(20):5807–5812.
20. Fracasso G, Bellisola G, Cingarlini S, Castelletti D, Prayer-Galetti T, Pagano F, Tridente G, Colombatti M. Anti-tumor effects of toxins targeted to the prostate specific membrane antigen. The Prostate 2002;53(1):9–23.
21. Wu LY, Anderson MO, Toriyabe Y, Maung J, Campbell TY, Tajon C, Kazak M, Moser J, Berkman CE. The molecular pruning of a phosphoramidate peptidomimetic inhibitor of prostate-specific membrane antigen. Bioorg Med Chem 2007; 15(23):7434–7443.
22. Ding P, Helquist P, Miller MJ. Design, synthesis and pharmacological activity of novel enantiomerically pure phosphonic acid-based NAALADase inhibitors. Org Biomol Chem 2007;5(5):826–831.
23. Majer P, Hin B, Stoermer D, Adams J, Xu W, Duvall BR, Delahanty G, Liu Q, Stathis MJ, Wozniak KM, Slusher BS, Tsukamoto T. Structural optimization of thiol-based inhibitors of glutamate carboxypeptidase II by modification of the P1′ side chain. J Med Chem 2006;49(10):2876–2885.
24. Aggarwal S, Singh P, Topaloglu O, Isaacs JT, Denmeade SR. A dimeric peptide that binds selectively to prostate-specific membrane antigen and inhibits its enzymatic activity. Cancer Res 2006;66(18):9171–9177.
25. Wone DW, Rowley JA, Garofalo AW, Berkman CE. Optimizing phenylethylphosphonamidates for the inhibition of prostate-specific membrane antigen. Bioorg Med Chem 2006;14(1):67–76.
26. Maung J, Mallari JP, Girtsman TA, Wu LY, Rowley JA, Santiago NM, Brunelle AN, Berkman CE. Probing for a hydrophobic a binding register in prostate-specific membrane antigen with phenylalkylphosphonamidates. Bioorg Med Chem 2004;12(18): 4969–4979.
27. Kozikowski AP, Zhang J, Nan F, Petukhov PA, Grajkowska E, Wroblewski JT, Yamamoto T, Bzdega T, Wroblewska B, Neale JH. Synthesis of urea-based inhibitors as active site probes of glutamate carboxypeptidase II: Efficacy as analgesic agents. J Med Chem 2004;47(7):1729–1738.
28. Oliver AJ, Wiest O, Helquist P, Miller MJ, Tenniswood M. Conformational and SAR analysis of NAALADase and PSMA inhibitors. Bioorg Med Chem 2003;11(20):4455–4461.
29. Stoermer D, Liu Q, Hall MR, Flanary JM, Thomas AG, Rojas C, Slusher BS, Tsukamoto T. Synthesis and biological evaluation of hydroxamate-Based inhibitors of glutamate carboxypeptidase II. Bioorg Med Chem Lett 2003;1313:2097–2100.
30. Majer P, Jackson PF, Delahanty G, Grella BS, Ko YS, Li W, Liu Q, Maclin KM, Polakova J, Shaffer KA, Stoermer D, Vitharana D, Wang EY, Zakrzewski A, Rojas C, Slusher BS, Wozniak KM, Burak E, Limsakun T, Tsukamoto T. Synthesis and biological evaluation of thiol-based inhibitors of glutamate carboxypeptidase II: Discovery of an orally active GCP II inhibitor. J Med Chem 2003;4610:1989–1996.
31. Jackson PF, Cole DC, Slusher BS, Stetz SL, Ross LE, Donzanti BA, Trainor DA. Design, synthesis, and biological activity of a potent inhibitor of the neuropeptidase N-acetylated alpha-linked acidic dipeptidase. J Med Chem 1996;39(2):619–622.
32. Serval V, Barbeito L, Pittaluga A, Cheramy A, Lavielle S, Glowinski J. Competitive inhibition of N-acetylated-alpha-linked acidic dipeptidase activity by N-acetyl-L-aspartyl-beta-linked L-glutamate. J Neurochem 1990;55(1):39–46.
33. Zhou J, Neale JH, Pomper MG, Kozikowski AP. NAAG peptidase inhibitors and their potential for diagnosis and therapy. Nat Rev Drug Discov 2005;4(12):1015–1026.
34. Tang H, Brown M, Ye Y, Huang G, Zhang Y, Wang Y, Zhai H, Chen X, Shen TY, Tenniswood M. Prostate targeting ligands based on N-acetylated alpha-linked acidic dipeptidase. Biochem Biophys Res Commun 2003;307(1):8–14.
35. Jayaprakash S, Wang X, Heston WD, Kozikowski AP. Design and synthesis of a PSMA inhibitor-doxorubicin conjugate for targeted prostate cancer therapy. ChemMedChem 2006;1(3): 299–302.
36. Wu LY, Do JC, Kazak M, Page H, Toriyabe Y, Anderson MO, Berkman CE. Phosphoramidate derivatives of hydroxysteroids as inhibitors of prostate-specific membrane antigen. Bioorg Med Chem Lett 2008;18(1):281–284.
37. Anderson MO, Wu LY, Santiago NM, Moser JM, Rowley JA, Bolstad ES, Berkman CE. Substrate specificity of prostate-specific membrane antigen. Bioorg Med Chem 2007;15(21): 6678–6686.
38. Liu T, Toriyabe Y, Berkman CE. Purification of prostate-specific membrane antigen using conformational epitope-specific antibody-affinity chromatography. Protein Expr Purif 2006;49(2): 251–255.
39. Tino WT, Huber MJ, Lake TP, Greene TG, Murphy GP, Holmes EH. Isolation and characterization of monoclonal antibodies specific for protein conformational epitopes present in prostate-specific membrane antigen (PSMA). Hybridoma 2000;19(3):249–257.
40. Rajasekaran SA, Anilkumar G, Oshima E, Bowie JU, Liu H, Heston W, Bander NH, Rajasekaran AK. A novel cytoplasmic tail MXXXL motif mediates the internalization of prostate-specific membrane antigen. Mol Biol Cell 2003;14(12):4835–4845.
41. Anilkumar G, Rajasekaran SA, Wang S, Hankinson O, Bander NH, Rajasekaran AK. Prostate-specific membrane antigen association with filamin A modulates its internalization and NAALADase activity. Cancer Res 2003;63(10):2645–2648.
42. Liu H, Rajasekaran AK, Moy P, Xia Y, Kim S, Navarro V, Rahmati R, Bander NH. Constitutive and antibody-induced internalization of prostate-specific membrane antigen. Cancer Res 1998; 58(18):4055–4060.
43. Mukherjee S, Ghosh RN, Maxfield FR. Endocytosis. Physiol Rev 1997;77(3):759–803.
44. van Renswoude J, Bridges KR, Harford JB, Klausner RD. Receptor-mediated endocytosis of transferrin and the uptake of fe in K562 cells: Identification of a nonlysosomal acidic compartment. Proc Natl Acad Sci USA 1982;79(20):6186–6190.
45. Klausner RD, Van Renswoude J, Ashwell G, Kempf C, Schechter AN, Dean A, Bridges KR. Receptor-mediated endocytosis of transferrin in K562 cells. J Biol Chem 1983;258(8):4715–4724.

46. Lamb JE, Ray F, Ward JH, Kushner JP, Kaplan J. Internalization and subcellular localization of transferrin and transferrin receptors in HeLa cells. J Biol Chem 1983;258(14):8751–8758.
47. Hopkins CR, Trowbridge IS. Internalization and processing of transferrin and the transferrin receptor in human carcinoma A431 cells. J Cell Biol 1983;97(2):508–521.
48. Dautry-Varsat A, Ciechanover A, Lodish HF. pH and the recycling of transferrin during receptor-mediated endocytosis. Proc Natl Acad Sci USA 1983;80(8):2258–2262.
49. Klausner RD, Harford J, van Renswoude J. Rapid internalization of the transferrin receptor in K562 cells is triggered by ligand binding or treatment with a phorbol ester. Proc Natl Acad Sci USA 1984;81(10):3005–3009.
50. Ghosh RN, Maxfield FR. Evidence for nonvectorial, retrograde transferrin trafficking in the early endosomes of HEp2 cells. J Cell Biol 1995;128(4):549–561.
51. Davis MI, Bennett MJ, Thomas LM, Bjorkman PJ. Crystal structure of prostate-specific membrane antigen, a tumor marker and peptidase. Proc Natl Acad Sci USA 2005;102(17):5981–5986.
52. Mesters JR, Barinka C, Li W, Tsukamoto T, Majer P, Slusher BS, Konvalinka J, Hilgenfeld R. Structure of glutamate carboxypeptidase II, a drug target in neuronal damage and prostate cancer. EMBO J 2006;25(6):1375–1384.
53. Robinson MB, Blakely RD, Couto R, Coyle JT. Hydrolysis of the brain dipeptide N-acetyl-L-aspartyl-L-glutamate. Identification and characterization of a novel N-acetylated alpha-linked acidic dipeptidase activity from rat brain. J Biol Chem 1987;26230: 14498–14506.
54. Pinto JT, Suffoletto BP, Berzin TM, Qiao CH, Lin S, Tong WP, May F, Mukherjee B, Heston WD. Prostate-specific membrane antigen: A novel folate hydrolase in human prostatic carcinoma cells. Clin Cancer Res 1996;2(9):1445–1451.
55. Barinka C, Rinnova M, Sacha P, Rojas C, Majer P, Slusher BS, Konvalinka J. Substrate specificity, inhibition and enzymological analysis of recombinant human glutamate carboxypeptidase II. J Neurochem 2002;80(3):477–487.
56. Yang J, Chen H, Vlahov IR, Cheng JX, Low PS. Characterization of the pH of folate receptor-containing endosomes and the rate of hydrolysis of internalized acid-labile folate-drug conjugates. J Pharmacol Exp Ther 2007;321(2):462–468.
57. Maxfield FR, McGraw TE. Endocytic recycling. Nat Rev Mol Cell Biol 2004;5(2):121–132.
58. Altan N, Chen Y, Schindler M, Simon SM. Defective acidification in human breast tumor cells and implications for chemotherapy. J Exp Med 1998;187(10):1583–1598.